



ELSEVIER

Contents lists available at ScienceDirect

## Journal of Physics and Chemistry of Solids

journal homepage: [www.elsevier.com/locate/jpcs](http://www.elsevier.com/locate/jpcs)

# The synthesis and photoelectric study of 6,13-bis(4-propylphenyl)pentacene, and its TiO<sub>2</sub> nano-sized composite films

Zhong Huang<sup>a</sup>, Yuansheng Jang<sup>c</sup>, Xiuying Yang<sup>b</sup>, Weiliang Cao<sup>a,b</sup>, Jingchang Zhang<sup>a,b,\*</sup>

<sup>a</sup> Institute of Modern Catalysis, State Key Laboratory of Chemical Resource Engineering, Beijing University of Chemical Technology, Beijing 100029, China

<sup>b</sup> Hainan Institute of Science and Technology, Haikou 571126, China

<sup>c</sup> School of Chemistry and Chemical Engineering, Nanjing University, Nanjing 210093, China

## ARTICLE INFO

### Article history:

Received 17 July 2009

Received in revised form

21 December 2009

Accepted 22 December 2009

### Keywords:

A. Electronic materials

B. Chemical synthesis

D. Electrical properties

## ABSTRACT

The synthesized 6,13-bis(4-propylphenyl)pentacene(BPP) is much more soluble and stable than pentacene. The introduction of 4-propylphenyl group leads the solubility to 7.33 mg/mL in CHCl<sub>3</sub>. In cyclic voltammetry (CV) test, it was found that its forbidden band gap is 1.88 eV. Moreover, a series of BPP–TiO<sub>2</sub> composites were constructed. Characterizations proved that an interaction between BPP and TiO<sub>2</sub> has probably occurred, leading to the generation of some novel properties. The most interesting result is that the forbidden band gaps of the composite materials are much smaller than that of BPP and TiO<sub>2</sub>.

© 2010 Elsevier Ltd. All rights reserved.

## 1. Introduction

Pentacene as one of the most important candidate for organic semiconductor in electronic devices has been paid much attention in the past decades [1–3], but its poor solubility and stability limit its large-scale application. Actually, some efforts have been made to overcome these demerits, leading to many new pentacene derivatives [4–12]. However, most of these researches are only focused on pentacenes themselves, and these pentacenes as p-type semiconductors cannot overcome the poor conductivity in reduction potential.

Organic–inorganic composite has attracted continuous attention because of its remarkable properties [13]. One of these composites is nano-scaled core-shell materials consisting of oxide particles and a functional organic shell. The material may offer a great potential for improving the novel electrical and optical properties. It was expected that when pentacenes coat nano-materials, the charge distribution of their atoms, the molecular stacking, the lowest unoccupied molecular orbital (LUMO) level, the highest occupied orbital (HOMO) level, and forbidden band gap could be changed.

In this paper, we would like to report a new synthesized 6,13-bis(4-propylphenyl)pentacene (BPP) and its composites with nano-sized TiO<sub>2</sub> on the basis of our former works [9]. BPP has much better solubility and stability than pentacene. It was indeed

found that after the composite of BPP with TiO<sub>2</sub>, the composite BPP–TiO<sub>2</sub> materials have different optical and electrical performance. The most interesting result is that the forbidden band gaps of the composite materials are much smaller than those of both BPP and TiO<sub>2</sub>, and these materials could overcome disadvantages of the poor conductivity at reduction potential of BPP and the poor conductivity at oxidation region of nano-sized TiO<sub>2</sub>.

## 2. Experiment

### 2.1. Apparatus for measurements

<sup>1</sup>H NMR spectra were recorded with Bruker, AV 600 NMR spectrometer in CDCl<sub>3</sub>. Elemental analysis was conducted on a Vario EL elemental analyzer. Infrared spectra were recorded by a prestige-211R spectrophotometer in KBr flake. Cyclic voltammetry (CV) was performed on an IM6e Electrochemical Station. UV–vis absorption spectra and experiment on stability were measured on a UV-2501PCS double spectrophotometer. The fluorescence spectra (CHCl<sub>3</sub> solution) were obtained with a Shimadzu RF-5301PC spectrophotometer. Melting point was measured on X-4 binocular melting point measurement apparatus. X-ray photoelectron spectroscopy (XPS) was characterized on ESCALAB 250.

### 2.2. Synthesis of BPP

Fig. 1 shows the synthetic procedure. A solution of 4-propyl-1-bromobenzene (5 ml, 32 mmol) in THF (7 mL) was added to the

\* Corresponding author. Tel./fax: +86 01 64434904.

E-mail address: zhangjc1@mail.buct.edu.cn (J. Zhang).

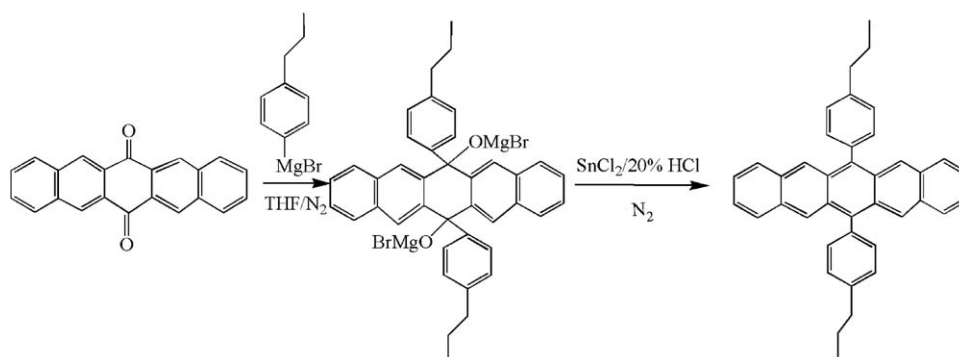


Fig. 1. Synthesis of 6, 13-bis(propylphenyl)pentacene.

nitrogen-purged mixture of dried Mg powder (0.77 g, 32.1 mmol) in THF (5 mL) at room temperature to synthesize the Grignard reagent. The reaction system was stirred for 30 min. The suspension of 6,13-pentacenequinone (1.0 g, 3.2 mmol) in THF (20 mL) was added slowly on ice bath, and the system was then heated to 60 °C for 1 h. After cooling to room temperature, a mixture of 20% HCl (30 mL) saturated with SnCl<sub>2</sub> was added very carefully. The reaction was heated at 60 °C for 2 h, followed by cooling to room temperature. The mixture was filtered, and the purple cake as crude product was washed with water (5 mL × 3), ethanol (5 mL × 3) and diethyl ether (5 mL × 3), respectively. After drying in vacuum, the crude product was purified by column chromatography using petroleum ether/CHCl<sub>3</sub> (20:1) as eluent and silica gel as sorbent. The solvents were removed in vacuo and the purple-red powder product yielded 44.3%. During the isolation process, light was avoided.

### 2.3. Preparation of BPP–TiO<sub>2</sub> nano-composite

BPP (0.063 mmol) in CHCl<sub>3</sub> (2 mL), and nano-sized TiO<sub>2</sub> (about 8 nm, 1–10 equiv.) were added into a sealed flask. The system was processed by ultrasound irradiation for 3 h, and CHCl<sub>3</sub> was then instantly removed by vacuum to give BPP–TiO<sub>2</sub> nano-composite. Noticeably, light must be avoided in the process.

### 2.4. Preparation of BPP and composite films

After ultrasound process, the suspension was evenly dropped to ITO and quartz glass instantly. After CHCl<sub>3</sub> was evaporated, two films were prepared. The film on ITO was used to get cyclic voltammetry, and the other was used for UV–vis spectra, and fluorescence spectra. BPP film was prepared by the same way except ultrasound process.

### 2.5. Electrochemical measurements by cyclic voltammetry

Cyclic voltammetry (CV) was performed on an IM6e Electrochemical Station (ZAHNER ELEKTRIK), with a scanning rate of 150 mV/s. The CV studies of pentacenes were carried out in acetonitrile with 0.1 M LiClO<sub>4</sub>, using Pt wires and 0.01 M Ag/AgNO<sub>3</sub> in acetonitrile as electrodes. The values are expressed in potentials versus Fc/Fc<sup>+</sup>. All solutions were insufflated with N<sub>2</sub> for 30 min.

Table 1  
Solubility of BPP and pentacene (20 °C).

Compounds	Solubility (mg mL <sup>-1</sup> )			
	CHCl <sub>3</sub>	THF	DMF	Toluene
Pentacene	0.21	0.11	0.10	0.18
BPP	7.33	2.25	0.52	5.00

## 3. Results and discussion

### 3.1. Configuration characterizations of BPP

The characteristic signals of <sup>1</sup>H NMR spectra of as-obtained BPP are displayed as follows (in ppm unit): 1.14 (t, 6H), 1.90 (m, 4H), 2.86 (t, 4H), 7.22(m, 4H), 7.52(m, 8H), 7.73(d, 4H), 8.34(s, 4H). FT-IR (cm<sup>-1</sup>): 3042, 2957, 2925, 2857, 1460, 876, 825, 802, 743. The result of elemental analysis is that the contents are 93.40% (C) and 6.54% (H), very approximate to the theoretical values of 93.34% (C) and 6.66% (H). M.P.: 185.7–187.7 °C (decomposition).

### 3.2. Solubility of BPP

Table 1 shows the solubilities of BPP and pentacene [9] in some common organic solvents. The solubility of BPP was largely enhanced after the introduction of 4-propylphenyl group, which is caused by the fact that 4-propylphenyl group largely enhances steric hindrance and reduces the strong force between pentacene backbones. However, BPP still has the same soluble trend with that of pentacene.

### 3.3. UV–vis and fluorescence spectra of BPP

Fig. 2 shows three absorption peaks at 518, 557, and 602 nm of BPP in CHCl<sub>3</sub>, and the absorption becomes stronger in order. The molar absorptivities at the three wavelengths are 512, 1128, and 1568 M<sup>-1</sup> cm<sup>-1</sup>, which show its good absorption. Its maximum absorption wavelength (λ<sub>max</sub>) is 602 nm, which only has a red shift of 2 nm compared with 6,13-diphenylpentacene (DPP) [9]. The reason is that the electron-donating ability of propyl group is so weak that its effect becomes very limited. However, BPP has a large red shift of 25 nm compared with pentacene (λ<sub>max</sub>=577 nm), which can be explained by the increased delocalization of π electrons after the introduction of 4-propylphenyl group. According to the onset absorption edge in visible light, the optical forbidden band gap (E<sub>g1</sub>) of BPP is calculated to be 2.00 eV, smaller than 2.02 eV of DPP [9]. Fluorescence spectrum (Fig. 2) shows the emitting peak of BPP is at 621 nm, with a Stokes shift of 19 nm.

### 3.4. Research on stability of BPP

Fig. 3 records the IR spectra of BPP exposure to the ambient light in air. The result shows that as the exposure time passed, no obvious change of BPP was observed. Therefore, BPP is very stable to ambient light and air.

In order to get information about BPP's stability, our group adopted a very detailed measurement. Four decomposition processes (a, b, c, d) of BPP in  $\text{CHCl}_3$  are shown in Fig. 4. Under condition a, the half life of BPP is 13 min, and under condition b, the half life is 34 min. However, under conditions c and d, the color of solution could be retained for weeks. At last, three results can be concluded from the processes as follows: (1) The new pentacene is sensitive to light in solution. (2) It is more sensitive to light than to oxygen, and its decomposition is mainly caused by light. (3) When combined with light, oxygen can accelerate its decomposition, but the effect of oxygen is very limited without light. BPP is much more stable than pentacene (about 3 min of half life at the same condition). The factor may be that (1) BPP has larger steric hindrance in 6,13 positions, and molecules of BPP are more difficult to be attacked by  $\text{O}_2$ . (2) The substituent decreases

the electron density of pentacene backbone through the  $\pi$ - $\pi$  conjugation.

### 3.5. XRD of BPP-TiO<sub>2</sub> nano-composites

Fig. 5 shows XRD spectra of BPP, BPP-TiO<sub>2</sub> composites and nano-sized TiO<sub>2</sub>. BPP has a good crystal form, with main diffraction peaks at 5–30°. Sharp diffraction peaks appear at 18.44°, 21.04°, and 26.32°. After coating on nano-sized TiO<sub>2</sub>, the crystal form of BPP slowly disappears as the mol ratio becomes smaller, such as its characteristic peaks at 18.44° and 21.04°. Instead of these peaks, a broad peak at 15–25° appears, which derives from the destroying of BPP molecular stacking after coating nano-TiO<sub>2</sub>. At the mol ratio of 1:5, BPP characteristics fully disappear. The crystal form of TiO<sub>2</sub> is not obviously changed after being coated by BPP, but 2 $\theta$  of all peaks increases by one degree, leading to a smaller interplanar spacing of TiO<sub>2</sub>. The transfer of electrons from BPP to TiO<sub>2</sub> may give an explanation. After acceptance of  $\pi$  electrons, the electric density of Ti increases, while O with a good electric affinity can attract  $\pi$  electrons from

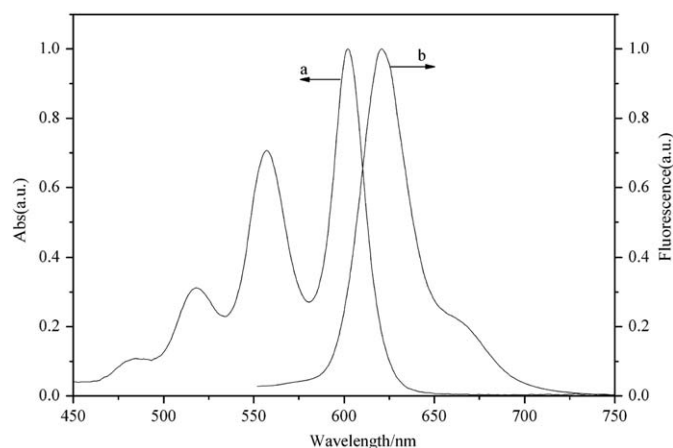


Fig. 2. (a) UV-vis spectra and (b) fluorescence spectra ( $\lambda_{\text{ex}}=532$  nm) of BPP in  $\text{CHCl}_3$ .

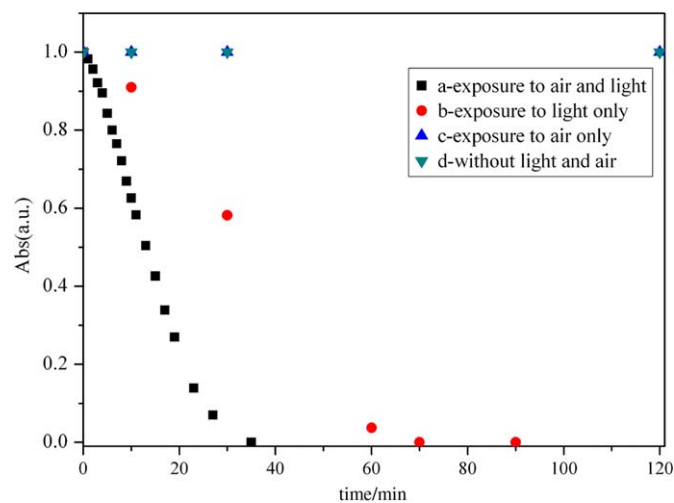


Fig. 4. Different oxidative processes of the BPP- $\text{CHCl}_3$  solution under different conditions.

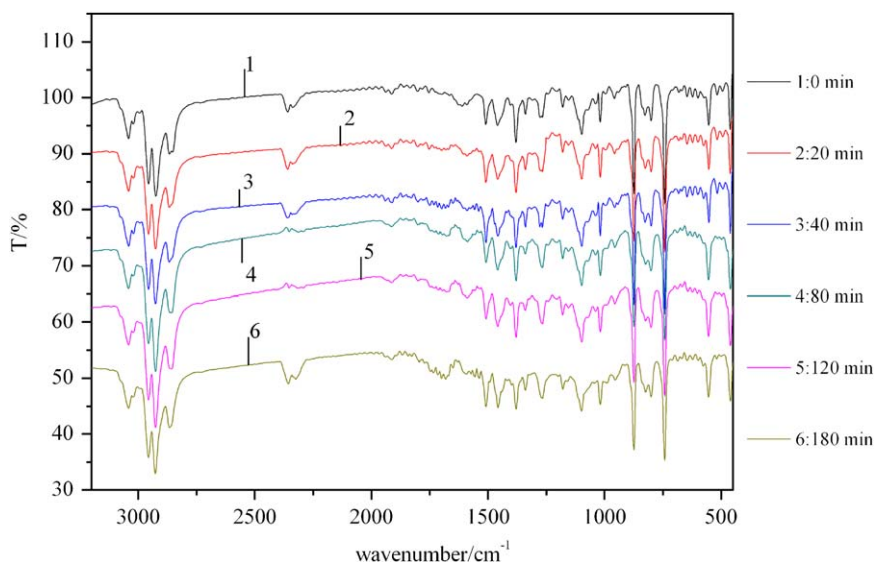


Fig. 3. IR spectra of BPP (solid states) exposure to ambient and strong light.

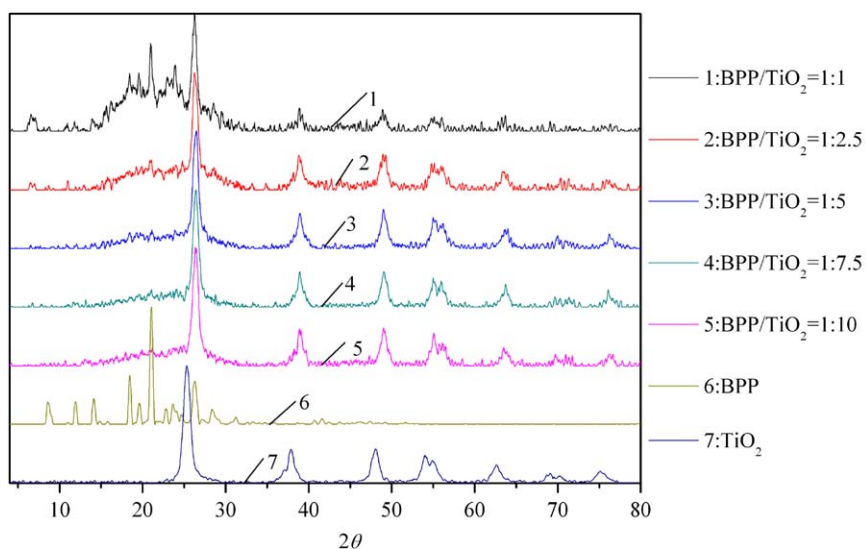


Fig. 5. XRD spectra of BPP, BPP-TiO<sub>2</sub>, and TiO<sub>2</sub>.

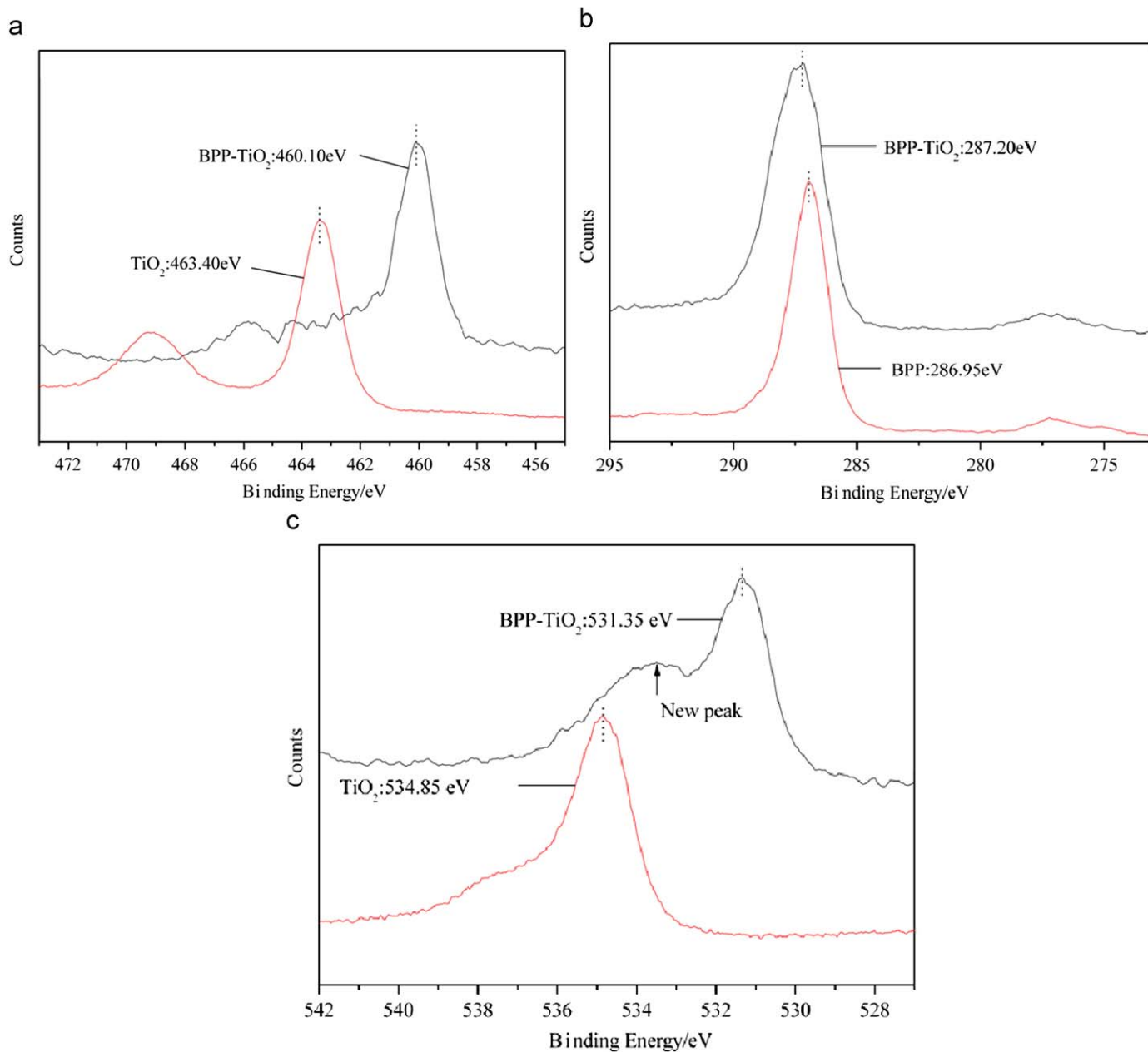


Fig. 6. XPS spectra of: (a) Ti2p; (b) C1s and (c) O1s.

BPP through Ti. As a result, the Ti–O bond is strengthened, the bond length and interplanar spacing are shortened. XPS can further define the interaction.

### 3.6. XPS of BPP–TiO<sub>2</sub> nano-composites

Fig. 6 gives comparative XPS of Ti, C, and O without adjustment. The binding energy of Ti decreases from 463.40 to 460.10 eV, and that of O decreases from 534.85 to 531.35 eV. The result shows that the two elements accept electrons after composition to give decreased valence states. Inversely, the binding energy of C of BPP increases from 286.95 to 287.20 eV, which shows C lost electrons to result in increased valence state. Another important information is that shoulder peak at 533.49 eV for O XPS appears after composition, which indicates the splitting valence for O, and not all of oxygen atoms have the same  $\pi$  electrons. It is well known that titanium (IV) with 5 empty orbits is a strong Lewis acid, and easy to accept electrons, while BPP is rich in delocalized  $\pi$  electrons, and easy to donor electrons.

Therefore,  $\pi$  electrons of BPP are inclined to transfer to TiO<sub>2</sub>, and a  $\pi \rightarrow d$  interaction may happen.

### 3.7. IR spectra

Fig. 7 gives IR spectra of BPP, BPP–TiO<sub>2</sub> nano-composites, and TiO<sub>2</sub>. Three peaks at 700–800 cm<sup>-1</sup>, belonging to the out-of-plane bending of C–H in C=C and the characteristic peaks of aromatic rings, disappear gradually, and peaks at the region fully disappear at a mol ratio of 1:5. The disappearance indicates the complete composition of BPP molecules and nano-sized TiO<sub>2</sub>, and that the coating of BPP at nano-sized TiO<sub>2</sub> hinders these vibrations. Additionally, peak at 1277 cm<sup>-1</sup> belonging to the in-plane bending vibration of C–H bond of pentacene framework sharply strengthens, while peak at 876 cm<sup>-1</sup> belonging to out-of-plane bending of C–H suddenly weakens. These obvious changes confirm that the interaction existed between BPP and nano-sized TiO<sub>2</sub>.

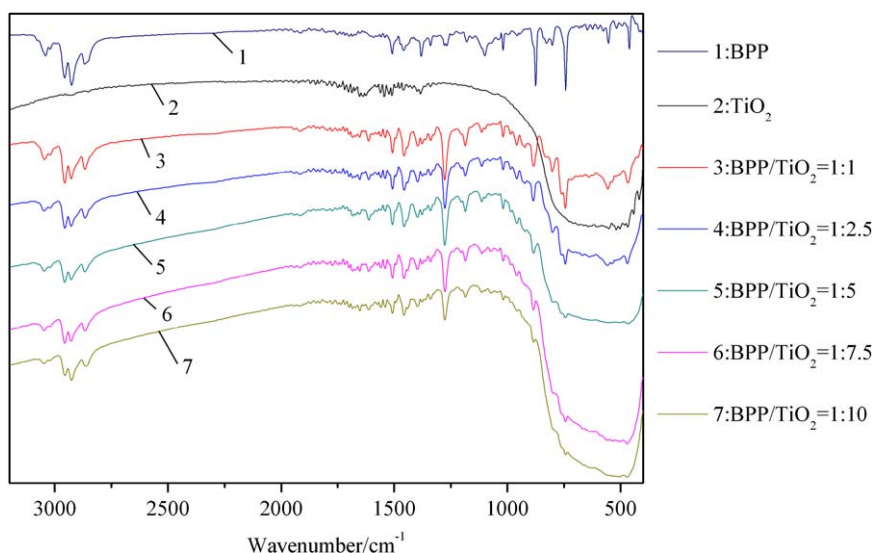


Fig. 7. IR spectra of BPP, BPP–TiO<sub>2</sub> and TiO<sub>2</sub>.

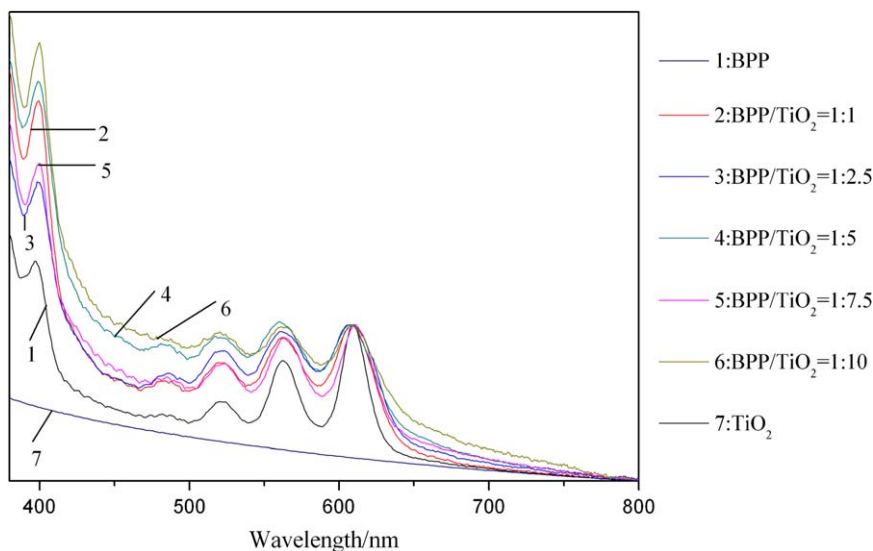


Fig. 8. UV–vis absorption spectra of BPP, BPP–TiO<sub>2</sub> and TiO<sub>2</sub>.

### 3.8. UV-vis absorption and fluorescence spectra of BPP-TiO<sub>2</sub> nano-composites film

Fig. 8 gives UV-vis spectra of BPP, BPP-TiO<sub>2</sub> nano-composites, and nano-sized TiO<sub>2</sub>. The ability of absorbing UV-vis light was enhanced after composition, especially at the region under 450 nm. Peaks at 610, 562, and 520 nm of BPP had shifts of 2–5 nm. The phenomenon may be caused by  $\pi \rightarrow d$  coordination interaction between BPP and nano-sized TiO<sub>2</sub>. Fluorescence spectra (Fig. 9) show that on the influence of nano-sized TiO<sub>2</sub>, the main emitting peak at 607 nm changed little, but new emitting peaks at 634 and 666 nm appeared. The conclusion can also confirm the interaction between BPP and nano-sized TiO<sub>2</sub> (Fig. 10).

### 3.9. CV of BPP-TiO<sub>2</sub> nano-composites film

Table 2 exhibits CV data of BPP, BPP-TiO<sub>2</sub> nano-composites, and nano-sized TiO<sub>2</sub>. From the onset oxidation potential ( $E_{\text{ox}}^{\text{onset}}$ ) and the onset reduction potential ( $E_{\text{red}}^{\text{onset}}$ ), the electric forbidden band gap ( $E_{g2}$ ) of BPP is 1.88 eV.  $E_{g2}$  for composites were calculated to be 1.14–1.35 eV, much smaller than those of BPP and TiO<sub>2</sub>. The change of  $E_{\text{red}}^{\text{onset}}$  further confirms the interaction between BPP and nano-sized TiO<sub>2</sub>. However, no obvious change for  $E_{\text{ox}}^{\text{onset}}$  is found. The reason may be that the difference between HOMO levels of BPP and nano-TiO<sub>2</sub> is too big to match (Fig. 11), but their LUMO levels are so approximate that the match happens

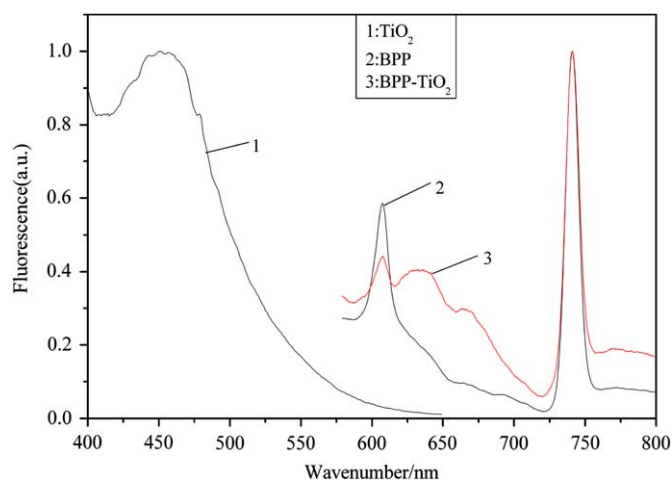


Fig. 9. Fluorescence spectra of BPP (excited by 490 nm), BPP-TiO<sub>2</sub> (in mol ratio of 1:5, excited by 490 nm) and TiO<sub>2</sub> (excited by 360 nm).

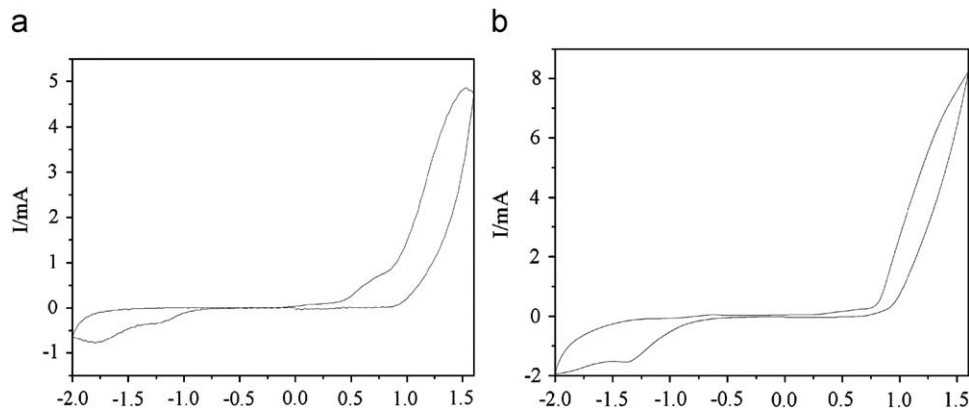


Fig. 10. CV of: (a) BPP and (b) BPP-TiO<sub>2</sub> (in mol ratio of 1:5).

easily. Additionally, the ratio of the gross charge at the reduction potentials and the gross charge at the oxidation potentials ( $Q_{\text{red}}/Q_{\text{ox}}$ ) became larger, and the characteristics for n semiconductors were more obvious as the mol ratio of BPP and nano-TiO<sub>2</sub> was smaller. It can be concluded that these new composites have the mixed property of n and p semiconductors.

## 4. Conclusions

(1) The new pentacene in CHCl<sub>3</sub> has a maximum absorption peak at 602 nm, and a maximum emitting peak at 621 nm. (2) XRD shows that BPP has a good crystal form. Owing to the good stacking, its forbidden band gap is 1.88 eV. (3) BPP is much more

Table 2  
Electrochemical data for BPP, BPP-TiO<sub>2</sub>, and TiO<sub>2</sub>.

BPP/TiO <sub>2</sub> (in mol ratio)	<sup>a</sup> $E_{\text{ox}}^{\text{onset}}$ (V)	<sup>b</sup> $E_{\text{HOMO}}$ (eV)	<sup>a</sup> $E_{\text{red}}^{\text{onset}}$ (V)	<sup>b</sup> $E_{\text{LUMO}}$ (eV)	<sup>c</sup> $E_{g2}$ (eV)	$Q_{\text{red}}/Q_{\text{ox}}$
BPP	0.40	-5.11	-1.44	-3.27	1.88	-
1:1	0.42	-5.13	-0.72	-3.99	1.14	0.152
1:2.5	0.47	-5.18	-0.75	-3.96	1.22	0.227
1:5	0.35	-5.06	-0.88	-3.83	1.23	0.478
1:7.5	0.32	-5.03	-1.02	-3.69	1.34	0.585
1:10	0.47	-5.18	-0.88	-3.83	1.35	0.686
TiO <sub>2</sub>	2.14	-6.85	-0.94	-3.77	3.08	-

<sup>a</sup>  $E_{\text{ox}}^{\text{onset}}$  and  $E_{\text{red}}^{\text{onset}}$  vs. 0.01 M Ag<sup>+</sup>/Ag in CH<sub>3</sub>CN.

<sup>b</sup>  $E_{\text{HOMO}}$  and  $E_{\text{LUMO}}$  calculated by  $E_{\text{HOMO}} = -(E_{\text{ox}}^{\text{onset}} + 4.71)$  eV;  $E_{\text{LUMO}} = -(E_{\text{red}}^{\text{onset}} + 4.71)$  eV.

<sup>c</sup>  $E_{g2}$  calculated by  $E_{g2} = E_{\text{ox}}^{\text{onset}} - E_{\text{red}}^{\text{onset}}$ .

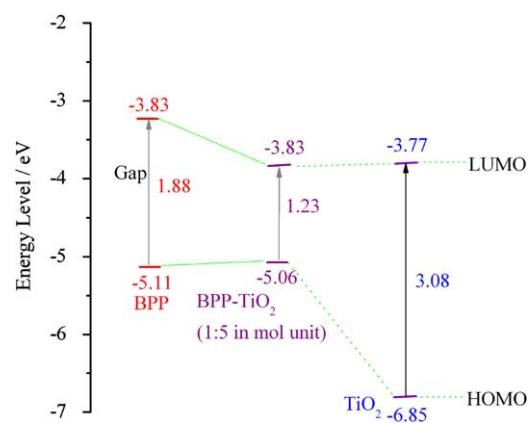


Fig. 11. Energy levels of BPP, BPP-TiO<sub>2</sub> (1:5 in mol ratio), and TiO<sub>2</sub>.

soluble and stable than pentacene, and particularly stable in solid state. The property provides the basis for its easy use in preparing composites and electronic devices. (4) BPP–TiO<sub>2</sub> nano-composites are new materials with smaller forbidden band gaps than those of BPP and nano-sized TiO<sub>2</sub>, which may be derived from the possible  $\pi \rightarrow d$  coordination between the two compounds. Compared with p semiconductor of BPP,  $E_{LUMO}$  was largely decreased to make electrons flow through more easily. Compared with n semiconductor of nano-sized TiO<sub>2</sub>,  $E_{HOMO}$  was largely enhanced to make pore generate more easily, which influences the composites to show better conductivity.

### Acknowledgements

The work was supported by the National High Technology Research and Development Program of China (863 Program, Grant no. 2006AA03Z412), and the National High Technology Research and Development Program of Hainan (Grant no. 509013).

### References

- [1] Y.Y. Lin, D.J. Gundlach, S. Nelson, T.N. Jackson, *IEEE Trans. Electron. Dev. Lett.* 18 (1997) 606.
- [2] M. Ahles, R. Schmechel, H. von Seggenrn, *Appl. Phys. Lett.* 85 (2004) 4499.
- [3] G. Bavdek, A. Cossaro, D. Cvetko, C. Africh, C. Blasetti, F. Esch, A. Morgante, L. Floreano, *Langmuir* 24 (2008) 767.
- [4] J.E. Anthony, *Chem. Rev.* 106 (2006) 5028.
- [5] Y.W. Zhao, R. Mondal, C.D. Neckers, *J. Org. Chem.* 73 (2008) 5506.
- [6] H.H. Huang, H.H. Hsieh, C.C. Wu, C.C. Lin, P.T. Chou, T.H. Chuang, Y.S. Wena, T.J. Chow, *Tetrahedron Lett.* 49 (2008) 4494.
- [7] Y.N. Li, Y.L. Wu, P. Liu, Z. Prostran, S. Gardner, B.S. Ong, *Chem. Mater.* 19 (2007) 418.
- [8] J.Y. Jiang, B.R. Kaafarani, D.C. Neckers, *J. Org. Chem.* 71 (2006) 2155.
- [9] (a) Y.L. Fu, J.C. Zhang, T. Zeng, Z. Huang, W.L. Cao, *Chin. Sci. Bull.* 53 (2008) 2607; (b) Z. Huang, Y.S. Jiang, X.Y. Yang, Y.L. Fu, W.L. Cao, J.C. Zhang, *Synth. Met.* 159 (2009) 1552.
- [10] B.B. Jang, S.H. Lee, Z.H. Kafafi, *Chem. Mater.* 18 (2006) 449.
- [11] Q. Miao, X. Chi, S. Xiao, R. Zeis, M. Lefenfeld, T. Siegrist, M.L. Steigerwald, C. Nuckolls, *J. Am. Chem. Soc.* 128 (2006) 1340.
- [12] E.J. Hwang, Y.E. Kim, C.J. Lee, J.W. Park, *Thin Solid Films* 499 (2006) 185.
- [13] (a) Y.H. Luo, J. Huang, I. Ichinose, *J. Am. Chem. Soc.* 127 (2005) 8296; (b) S. Shanmugam, B. Viswanathan, T.K. Varadarajan, *J. Membr. Sci.* 275 (2006) 105; (c) I. Zhitomirsky, *J. Alloys Compd.* 434, 435 (2006) 823.